A neuropeptide signaling pathway regulates synaptic growth in *Drosophila*

Xu Chen and Barry Ganetzky

Laboratory of Genetics, University of Wisconsin-Madison, Madison, WI 53706

Neuropeptide signaling is integral to many aspects of neural communication, particularly modulation of membrane excitability and synaptic transmission. However, neuropeptides have not been clearly implicated in synaptic growth and development. Here, we demonstrate that cholecystokinin-like receptor (CCKLR) and drosulfakinin (DSK), its predicted ligand, are strong positive growth regulators of the *Drosophila melanogaster* larval neuromuscular junction (NMJ). Mutations of *CCKLR* or *dsk* produced severe NMJ undergrowth, whereas overexpression of CCKLR caused overgrowth. Presynaptic expression of CCKLR was necessary and sufficient for regulating NMJ growth. *CCKLR* and *dsk* mutants also reduced synaptic function in parallel with decreased NMJ size. Analysis of double mutants revealed that DSK/CCKLR regulation of NMJ growth occurs through the cyclic adenosine monophosphate (cAMP)–protein kinase A (PKA)–cAMP response element binding protein (CREB) pathway. Our results demonstrate a novel role for neuropeptide signaling in synaptic development. Moreover, because the cAMP–PKA–CREB pathway is required for structural synaptic plasticity in learning and memory, DSK/CCKLR signaling may also contribute to these mechanisms.

Introduction

Proper synaptic growth is essential for normal development of the nervous system and its function in mediating complex behaviors such as learning and memory. The *Drosophila melanogaster* larval neuromuscular junction (NMJ) has become a powerful system for studying the molecular mechanisms underlying synaptic development and plasticity (Collins and DiAntonio, 2007), and many of the key synaptic proteins are evolutionarily conserved.

Genetic and molecular analysis in *Drosophila* has uncovered numerous molecules and pathways that regulate NMJ growth, including proteins required for cell adhesion, endocytosis, cytoskeletal organization, and signal transduction via TGF-β, Wingless, JNK, cAMP, and other signaling molecules (Featherstone and Broadie, 2000; Collins and DiAntonio, 2007). For example, previous studies revealed that increased cAMP levels led to a down-regulation of the cell adhesion protein FasII at synapses, and the activation of the cAMP response element binding protein (CREB) transcription factor to achieve long-lasting changes in synaptic structure and function (Davis et al., 1996; Schuster et al., 1996a,b). Despite the identification and characterization of these various positive and negative regulators, our understanding of the networks that govern synaptic growth is still incomplete, with many of the key components and mechanisms yet to be uncovered and analyzed.

To search for new regulators of synaptic growth, we conducted a forward genetic screen for mutants exhibiting altered NMJ morphology. In this screen, we discovered a new mutation that exhibits strikingly undergrown NMJs, which indicates disruption of a positive regulator of NMJ growth. We have identified the affected protein as cholecystokinin (CCK)-like receptor (CCKLR), a putative neuropeptide receptor that belongs to the family of G protein–coupled receptors (GPCRs) sharing a uniform topology with seven transmembrane domains. When activated by their ligands, neuropeptide GPCRs affect levels of second messengers such as cAMP, diacylglycerol, inositol trisphosphate, and intracellular calcium (Nässel, 2002). Through activation of their cognate receptors, secreted neuropeptides mediate communication among various sets of neurons as well

Correspondence to Barry Ganetzky: ganetzky@wisc.edu

Abbreviations used in this paper: AC, adenylyl cyclase; Brp, Bruchpilot; CCK, cholecystokinin; CCKLR, CCK-like receptor; CNS, central nervous system; CREB, cAMP-response element binding protein; DSK, drosulfakinin; EJP, excitatory junction potential; FaRP, FMRFamide-related peptide; GPCR, G protein–coupled receptor; mEJP, miniature EJP; NMJ, neuromuscular junction; rut, rutabaga; UAS, upstream activating sequence; WT, wild type.

The Rockefeller University Press $30.00
J. Cell Biol. Vol. 196 No. 4 529–543
www.jcb.org/cgi/doi/10.1083/jcb.201109044

as other cell types to regulate several physiological activities, including feeding and growth, molting, cuticle tanning, circadian rhythm, sleep, and learning and memory (Nässel and Winther, 2010). In general, neuropeptides act by modulating neuronal activity through both short-term and long-term effects. Short-term effects include modifications of ion channel activity and alterations in release of or response to neurotransmitters. Long-term effects include changes in gene expression through activation of transcription factors and protein synthesis. In contrast with the well-known effects of neuropeptide signaling on neuronal activity and the strength of synaptic transmission, regulation of synaptic growth and development by neuropeptides has not previously been clearly established.

Here, we demonstrate that CCKLR is required presynaptically to promote NMJ growth. Moreover, mutations of *drosulfakinin* (*dsk*), which encodes the predicted ligand of CCKLR, cause similar NMJ undergrowth and interact genetically with *CCKLR* mutations, indicating that DSK and CCKLR are components of a common signaling mechanism that regulates NMJ growth. In addition to the morphological phenotypes caused by mutations of *CCKLR* and *dsk*, mutant larvae also exhibit deficits in synaptic function. Through phenotypic analysis of double mutant combinations, we show that DSK/CCKLR signals through the cAMP–PKA–CREB pathway to regulate NMJ growth. Our results suggest a novel role for neuropeptide signaling in regulation of synaptic development. Moreover, because the cAMP-PKA-CREB pathway is required for structural plasticity of synapses in learning and memory, DSK/CCKLR signaling may also contribute to these mechanisms.

Results

Loss of *CCKLR* leads to NMJ undergrowth

To identify mutations that perturb synaptic growth and development, we used ethyl methanesulfonate for mutagenesis and screened directly for viable, X-linked mutants with aberrant larval NMJ morphology. One such mutant (referred to by its original isolation number, 88) exhibits striking NMJ undergrowth, with a 50% reduction in bouton number. In addition, the length of the NMJ branches is significantly reduced, and the boutons are enlarged (Fig. 1, A2 and B). Although we focused on the analysis of NMJ4 because of its relative simplicity, we observed similar phenotypes at NMJ6/7. The 88 mutation is recessive and localizes by deletion mapping to a small region (17D1-17D3) on the X chromosome (Fig. 1 E).

Df(1)Exel9051, which uncovers the mutant phenotype, removes ∼40 kb and spans only four genes. The biggest gene in this interval is *CCKLR-17D1*, which is predicted to encode a CCK-like neuropeptide receptor. The deficiency is sufficiently small that it is viable when hemizygous or homozygous, enabling us to examine NMJs of larvae completely lacking *CCKLR-17D1*. These larvae exhibit NMJ undergrowth very similar to that of 88 hemizygotes or homozygotes (Fig. 1, C1 and D), which indicates that 88 is a strong hypomorphic or null allele. Furthermore, we examined an insertional allele, $CCKLR\text{-}17D1^{MB02688}$ (referred to as $CCKLR^{Mi}$ for short), which carries a transposon inserted in the first intron (Fig. 1 E), and is thus presumed to be a weak hypomorph. Nonetheless, it failed to complement 88 (Fig. 1, A4 and B) and causes NMJ undergrowth when hemizygous (Fig. 1, C2, C3 and D). The undergrowth phenotype is stronger in $CCKLR^{Mi}/Df(1)Exel9051$ larvae, which is consistent with the prediction that $CCKLR^{Mi}$ is a hypomorphic allele (Fig. 1, C3 and D). We sequenced the entire *CCKLR-17D1* coding region in the 88 mutant but did not find any lesion. Thus, 88 most likely contains a regulatory mutation that interferes with expression of this gene. Because *Df(1)Exel9051* homozygotes are definitely null for *CCKLR-17D1*, we used these larvae (designated as $CCKLR\text{-}17D1^{\Delta}/Y$ or $CCKLR\text{-}17D1^{\Delta}/CCKLR\text{-}17D1^{\Delta}$) in subsequent experiments.

Because the *Drosophila* genome contains two *CCKLR* genes, *CCKLR-17D1* and *CCKLR-17D3*, separated by only ∼40 kb, we sought to determine whether *CCKLR-17D3* also affects NMJ growth. To answer this question, we used two different chromosomal duplications, *Dp(1;3)DC351* (designated as *Dp(17D1-D5)*) and *Dp(1;3)DC352* (designated as *Dp(17D3-E1)*), to rescue the NMJ phenotype of $CCKLR\text{-}17D1^{\Delta}/Y$. *Dp(17D1-D5)*, which contains a wild-type (WT) copy of both *CCKLR-17D1* and *CCKLR-17D3*, completely rescues NMJ undergrowth in $CCKLR\text{-}17D1^{\Delta}/Y$, as expected (Fig. S1, A3 and B). In contrast, *Dp(17D3-E1)*, which contains only a WT copy of *CCKLR-17D3*, fails to rescue $CCKLR\text{-}17D1^{\Delta}/Y$ (Fig. S1, A4 and B); this suggests that *CCKLR-17D3* cannot substitute for *CCKLR-17D1* in regulating NMJ growth. To test whether there is genetic interaction between these two CCKLRs, we used a deficiency, *Df(1)ED7413* (designated as *Df(17D1-F1)*), which removes both *CCKLR-17D1* and *CCKLR-17D3*. The NMJ phenotypes of *Df(17D1-F1)*/+ and $CCKLR\text{-}17D1^{\Delta}$/+ larvae do not differ (Fig. S1, C1 and D), which indicates that removing one copy of *CCKLR-17D3* does not further enhance the phenotype of $CCKLR\text{-}17D1^{\Delta}$/+ heterozygotes. Moreover, even in $CCKLR\text{-}17D1^{\Delta}/Df(17D1\text{-}F1)$ larvae, where one copy of *CCKLR-17D3* is removed in a *CCKLR-17D1*-null background, the NMJ phenotype is unchanged compared with *CCKLR-17D1*–null homozygotes (Fig. S1, C2 and D). We also examined an insertional allele of *CCKLR-17D3* ($CCKLR\text{-}17D3^{KG}$), and found no effect on NMJ growth in $CCKLR\text{-}17D3^{KG}$/Y or $CCKLR\text{-}17D3^{KG}/Df(17D1\text{-}F1)$ larvae (Fig. S1, C3, C4, and D). On the basis of these results, we conclude that *CCKLR-17D1* but not *CCKLR-17D3* is involved in regulating NMJ growth. We thus focus on *CCKLR-17D1*, hereafter referred to as *CCKLR* for short.

CCKLR functions presynaptically to regulate NMJ growth

Because neuropeptide signaling has not previously been characterized in synaptic development, it was of interest to determine where CCKLR function is required for proper NMJ growth. Neural-specific expression of RNAi directed against *CCKLR* using *C155-Gal4* resulted in NMJ undergrowth similar to the original mutant (Fig. 1, C4 and D). Conversely, rescue experiments using a series of different *Gal4* drivers demonstrated that presynaptic expression of *CCKLR* was sufficient to rescue the mutant phenotypes: Presynaptic expression of upstream activating sequence (UAS)-*CCKLR* using *C155-Gal4* substantially rescues the mutant phenotype of $CCKLR^{\Delta}/Y$ both for bouton number and

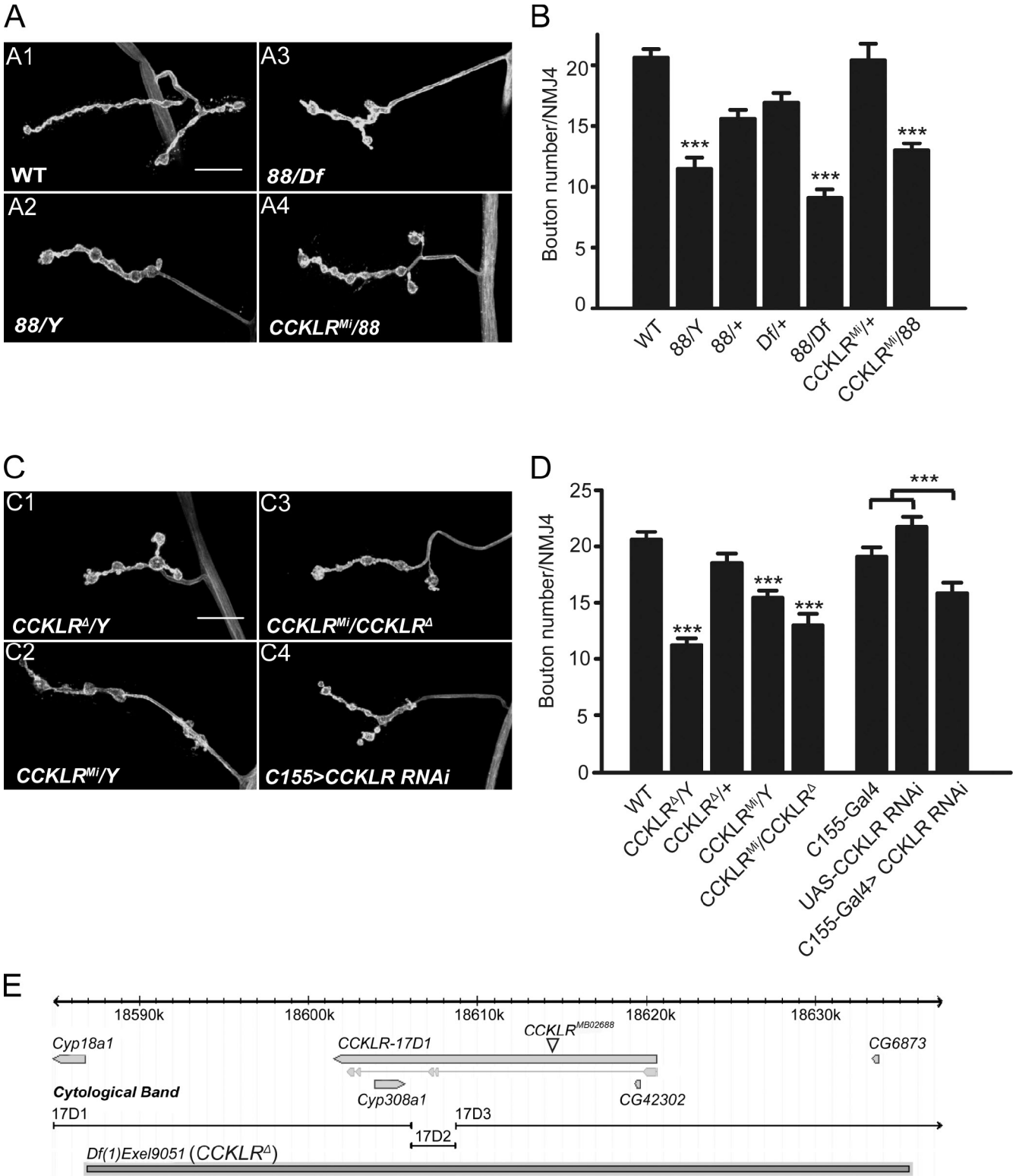

Figure 1. ***CCKLR* positively regulates NMJ growth in *Drosophila*.** (A and C) Confocal images of NMJ4 labeled with FITC–anti-HRP. (A) *88/Y*, *88/Df*, and *88/CCKLR^{Mi}* larvae all exhibit similar NMJ undergrowth compared with control. (B) Quantification of bouton numbers at NMJ4 for genotypes shown in A. *Df* shown in A and B is *Df(1)fu-A7*. (C) *CCKLR$^{\Delta}$/Y*, *CCKLR^{Mi}/Y*, *CCKLR^{Mi}/CCKLR-17D1$^{\Delta}$*, and *C155-Gal4>CCKLR* RNAi all exhibit similar NMJ undergrowth. Bars, 20 μM. (D) Quantification of bouton numbers at NMJ4 for genotypes shown in C. *CCKLR^{Mi}* is *CCKLR-17D1^{MB02688}*. *Df(1)Exel9051* is designated as *CCKLR$^{\Delta}$*. The genotype of *C155>CCKLR RNAi* larvae is *C155-Gal4 UAS-Dcr2/Y; UAS-CCKLR-RNAi^{7231}/+*. Error bars denote SEM. ***, $P < 0.001$ (compared with WT control unless indicated otherwise). (E) Gene structure and genomic view of *CCKLR-17D1* (modified from FlyBase.org).

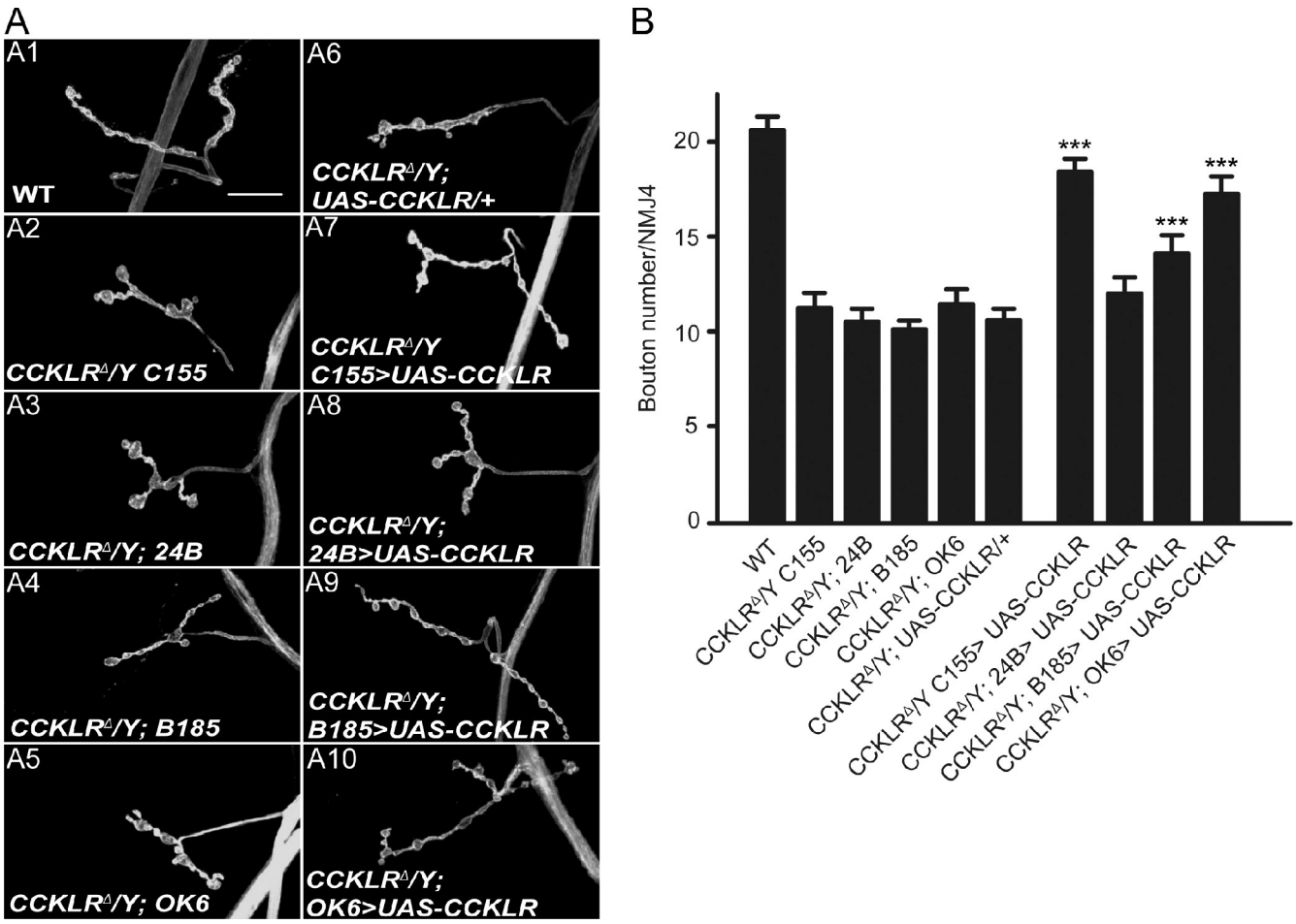

Figure 2. ***CCKLR* functions presynaptically to regulate NMJ growth.** (A) Confocal images of NMJ4 labeled with FITC–anti-HRP. Neuronal expression of *UAS-CCKLR* by *C155-Gal4* (A7) or *OK6-Gal4* (A10) in *CCKLR*$^{\Delta}$*/Y* background produces significant rescue of the NMJ undergrowth phenotype. Similar but less complete rescue is achieved when *UAS-CCKLR* is expressed under the control of *B185-Gal4* (A9), which drives expression both in motor neurons and in muscles. No rescue is seen when *24B-Gal4* is used to drive *UAS-CCKLR* in muscle (A8). Bar, 20 µm. (B) Quantification of bouton numbers at NMJ4 in larvae of the genotypes shown. The genotype of *CCKLR*$^{\Delta}$*/Y C155>UAS-CCKLR* is *C155-Gal4 CCKLR*$^{\Delta}$*/Y; UAS-CCKLR/+*. *CCKLR*$^{\Delta}$*/Y; OK6 >UAS-CCKLR* is *CCKLR*$^{\Delta}$*/Y; OK6-Gal4/UAS-CCKLR*. *CCKLR*$^{\Delta}$*/Y; 24B>UAS-CCKLR* is *CCKLR*$^{\Delta}$*/Y; UAS-CCKLR/+; 24B-Gal4/+*. *CCKLR*$^{\Delta}$*/Y; B185 >UAS-CCKLR* is *CCKLR*$^{\Delta}$*/Y; B185-Gal4/UAS-CCKLR*. Error bars denote SEM. ***, P < 0.001 (compared with corresponding *CCKLR*$^{\Delta}$*/Y; Gal4/+* and *CCKLR*$^{\Delta}$*/Y; UAS-CCKLR/+* controls).

overall NMJ morphology (17.9 ± 0.8 vs. 11.2 ± 0.8 boutons; Fig. 2, A7 and B), whereas postsynaptic expression via *24B-Gal4* has no significant effect on these phenotypes (12.0 ± 0.8 vs. 10.5 ± 0.7 boutons; Fig. 2, A8 and B). When we use *B185-Gal4* to drive *UAS-CCKLR* expression in all muscles and motor neurons (Davis et al., 1997), phenotypic rescue was not further increased beyond that observed with presynaptic expression alone (14.2 ± 0.9 vs. 10.1 ± 0.5 boutons; Fig. 2, A9 and B). The slight decrement in rescue with *B185-Gal4* compared with *C155-Gal4* is most likely caused by differences in the level of expression associated with the different drivers. We were also able to rescue *CCKLR*$^{\Delta}$*/Y* by driving *UAS-CCKLR* with *OK6-Gal4*, which is expressed preferentially in motor neurons (Fig. 2, A10 and B). Collectively, these data indicate that presynaptic *CCKLR* function is both necessary and sufficient to regulate NMJ growth.

Our efforts to raise a specific antibody against CCKLR to investigate its cellular localization were unsuccessful. As an alternative, we generated a tagged *UAS-CCKLR–mCherry* construct to examine the subcellular localization of CCKLR in neurons. Although *GAL4*-driven expression of this construct is not equivalent to the endogenous pattern of *CCKLR* expression, we found that it successfully rescued *CCKLR*$^{\Delta}$*/Y* when its expression was driven presynaptically by *C155-Gal4* (Fig. S2, A and B), which indicates that expression, subcellular localization, and function of the tagged protein overlap sufficiently well with that of endogenous CCKLR to confer a nearly normal phenotype. In these rescued larvae, CCKLR–mCherry is strongly expressed in cell bodies of motor neurons in the ventral ganglion (Fig. S2 C). Because *C155-Gal4* drives transcription pan-neuronally (unpublished data), the apparent enrichment of CCKLR–mCherry in motor neurons compared with other neurons in the ventral ganglion suggests that there are regulatory mechanisms that promote the translation or stabilization of CCKLR preferentially in motor neurons. We also detected CCKLR–mCherry in presynaptic boutons at NMJs, but the intensity is much lower than in cell bodies (Fig. S2 D). These results further suggest that CCKLR functions within motor neurons to regulate NMJ development.

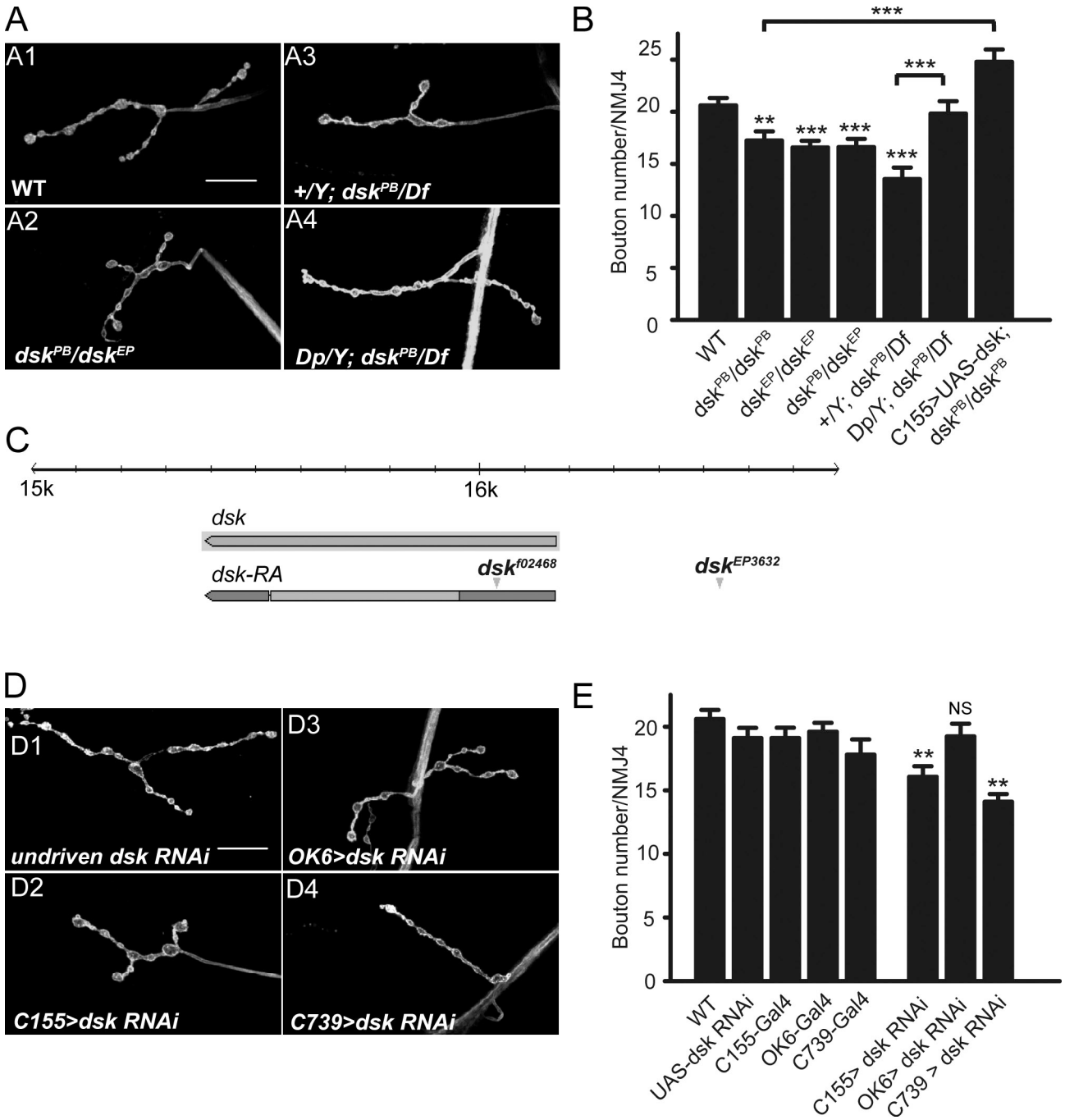

Figure 3. ***dsk* is a positive regulator of NMJ growth.** (A and D) Confocal images of NMJ4 labeled with FITC–anti-HRP. (A) dsk^{PB}/dsk^{EP} double heterozygotes (A2) and dsk^{PB}/Df larvae (A3) show NMJ undergrowth similar to *CCKLR* mutants. A duplicated genomic segment containing dsk^{+} inserted on the x chromosome rescues the phenotype of dsk^{PB}/Df (A4). (B) Quantification of bouton numbers at NMJ4 in *dsk* mutant larvae and rescued larvae. dsk^{PB} is dsk^{f02468}. dsk^{EP} is dsk^{EP3632}. *Df* is *Df(3R)2-2*. *Dp* is *Dp(3;1)2-2*. (C) Genomic organization of *dsk* showing sites of transposon insertion for two *dsk* mutations (modified from Flybase.org). (D) *dsk* RNAi driven by *C155-Gal4* (D2) and *C739-Gal4* (D4), but not *OK6-Gal4* (D3), leads to NMJ undergrowth. (E) Quantification of bouton numbers at NMJ4 for larvae shown in D. The genotype of *C155>dsk RNAi* larvae is *C155-Gal4 UAS-Dcr2/+; UAS-dsk-RNAi*^{14201}*/+*. *OK6>dsk RNAi* is *OK6-Gal4/+; UAS-dsk-RNAi*^{14201}*/+*. *C739>dsk RNAi* is *C739-Gal4/+; UAS-dsk-RNAi*^{14201}*/+*. Error bars denote SEM. ***, $P < 0.001$; **, $P < 0.01$ (compared with WT control unless indicated otherwise). Bars, 20 µm.

dsk interacts with *CCKLR* to regulate NMJ growth

Because neuropeptide receptors are typically activated in response to binding of specific neuropeptide ligands, we wished to determine if CCKLR's role in regulating NMJ growth was also ligand dependent. On the basis of sequence comparisons, the *Drosophila* orthologue of CCK is DSK, encoded by the *dsk* gene. Consequently, we examined the NMJ phenotype of two P-element insertion alleles, dsk^{f02468} (referred to as dsk^{PB}) and dsk^{EP3632} (referred to as dsk^{EP}; Fig. 3 C). Although neither mutation disrupts the coding region of *dsk*, both exhibited mild NMJ undergrowth as homozygotes or in heterozygous combination

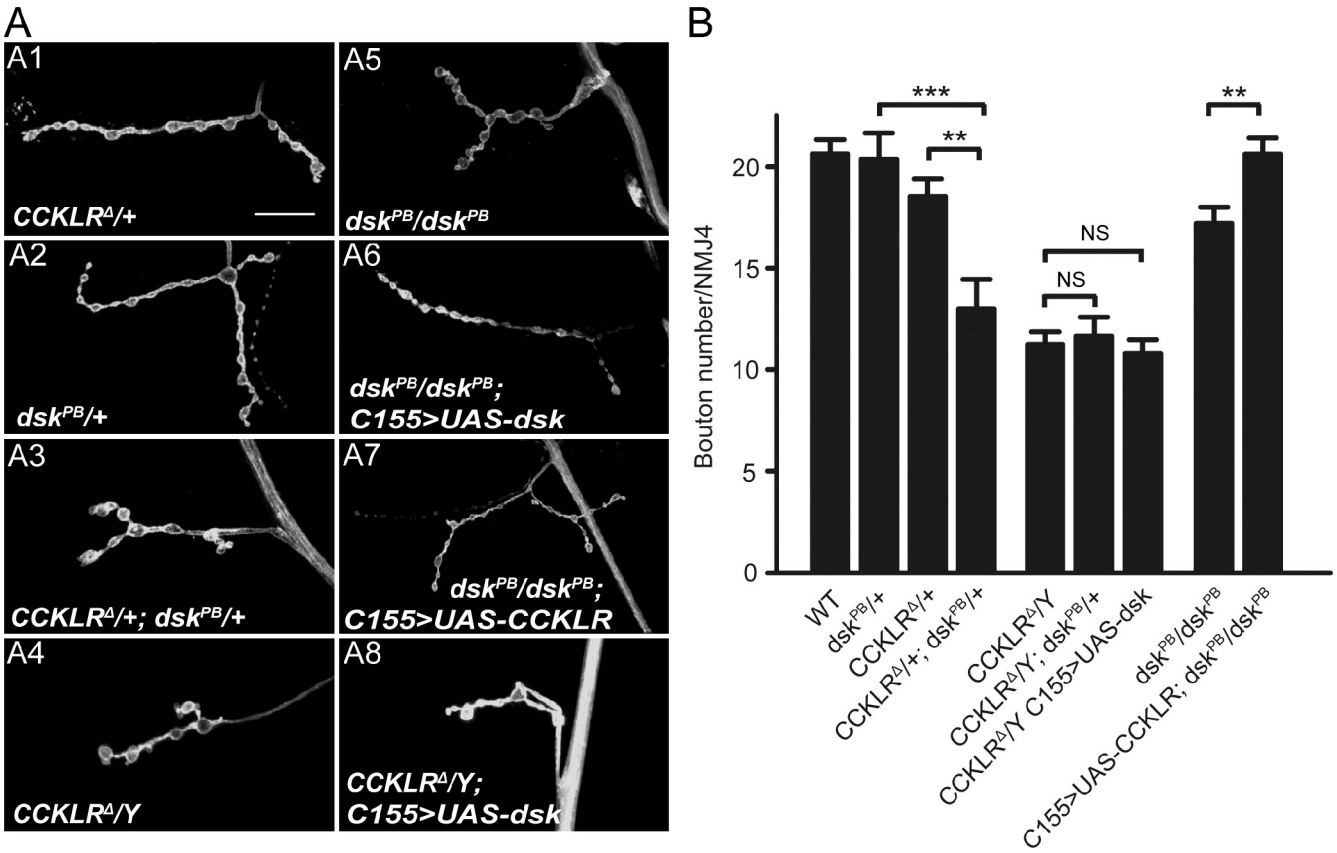

Figure 4. **Genetic interactions between *CCKLR* and *dsk*.** (A) Confocal images of NMJ4 labeled with FITC–anti-HRP. *CCKLR$^{\Delta}$/+; dsk^{PB}/+* double heterozygotes (A3) exhibit significantly enhanced NMJ undergrowth compared with either single heterozygote alone (A1 and A2). *C155-Gal4*–driven *UAS-dsk* rescues *dsk^{PB}/dsk^{PB}* (A6) but not *CCKLR$^{\Delta}$/Y* (A8). *C155-Gal4*–driven *UAS-CCKLR* overexpression also rescues *dsk^{PB}/dsk^{PB}* (A7). Bar, 20 µm. (B) Quantification of bouton numbers at NMJ4 in larvae of the genotypes shown in A. Error bars denote SEM. ***, $P < 0.001$; **, $P < 0.01$.

with each other (Fig. 3, A2 and B). Hemizygous *dsk^{PB}/Df(3R)2-2* larvae exhibit a more pronounced undergrowth phenotype, as expected, if the insertion is a weak hypomorphic allele (Fig. 3, A3 and B). The undergrowth phenotypes of *dsk^{PB}/Df(3R)2-2* or *dsk^{PB}/dsk^{PB}* are rescued by an X chromosome that carries an insertional duplication of a small segment of 3R that includes *dsk^{+}* (Fig. 3, A4 and B) or by *C155-Gal4*–driven expression of *UAS-dsk* (Fig. 3 B and Fig. 4 A6). Conversely, expression of *dsk* RNAi using the *C155-Gal4* driver results in NMJ undergrowth (Fig. 3, D2 and E). These results demonstrate that *dsk* is also a positive regulator of NMJ growth. Moreover, the NMJ undergrowth phenotype of *dsk* mutants is reminiscent of that observed in *CCKLR* mutants, which is consistent with the idea that DSK is the CCKLR ligand.

To determine where DSK is required for normal NMJ growth, we used different Gal4 drivers to express *UAS-dsk-RNAi*. *OK6-Gal4*–driven *dsk* RNAi in motor neurons does not cause the undergrowth phenotype that we observed with *C155-Gal4* (Fig. 3, D3 and E). In contrast, *UAS-dsk-RNAi* driven by *C739-Gal4* did result in significant NMJ undergrowth (Fig. 3, D4 and E). Although *C739-Gal4* is commonly used as a mushroom body driver (Tettamanti et al., 1997), it also drives expression in two longitudinal stripes in the ventral ganglion (Manseau et al., 1997) as well as in a group of neurosecretory cells, as revealed by *C739-Gal4*–driven *UAS-CD8–GFP* (Fig. S3). Compared with earlier immunohistochemical studies by Nichols (1992, 2003), it appears that *C739-Gal4* expression overlaps with DSK-positive cells (Fig. S3). Although at this point we do not know which specific groups of cells are required for DSK production, the results of these RNAi experiments suggest that DSK is not secreted by motor neurons, but instead is most likely secreted by neurosecretory cells in the central nervous system (CNS).

If DSK is the ligand for CCKLR and both of them affect the same pathway regulating NMJ growth, we might expect to observe phenotypic interactions between mutations that partially impair both *dsk* and *CCKLR*. In fact, whereas *CCKLR$^{\Delta}$*/+ alone (18.5 ± 0.8 boutons) or *dsk^{PB}*/+ heterozygotes alone (20.2 ± 1.3 boutons) do not significantly affect NMJ growth, the *CCKLR$^{\Delta}$*/+; *dsk^{PB}*/+ double heterozygotes exhibit a strong reduction in bouton number (13.0 ± 1.4; Fig. 4, A3 and B). In contrast, heterozygosity for *dsk^{PB}* does not further enhance the NMJ undergrowth phenotype of *CCKLR$^{\Delta}$/Y*-null mutants (Fig. 4 B), and *C155-Gal4*–driven overexpression of *UAS-dsk* is unable to rescue the *CCKLR$^{\Delta}$/Y*-null phenotype (Fig. 4, A8 and B). However, the NMJ undergrowth of homozygotes for *dsk^{PB}*, a hypomorphic *dsk* allele, is rescued by *C155-Gal4*–driven overexpression of *UAS-CCKLR* (Fig. 4, A7 and B). These results all support the idea that DSK and CCKLR are components of a common regulatory pathway affecting NMJ growth and that DSK is the ligand of CCKLR.

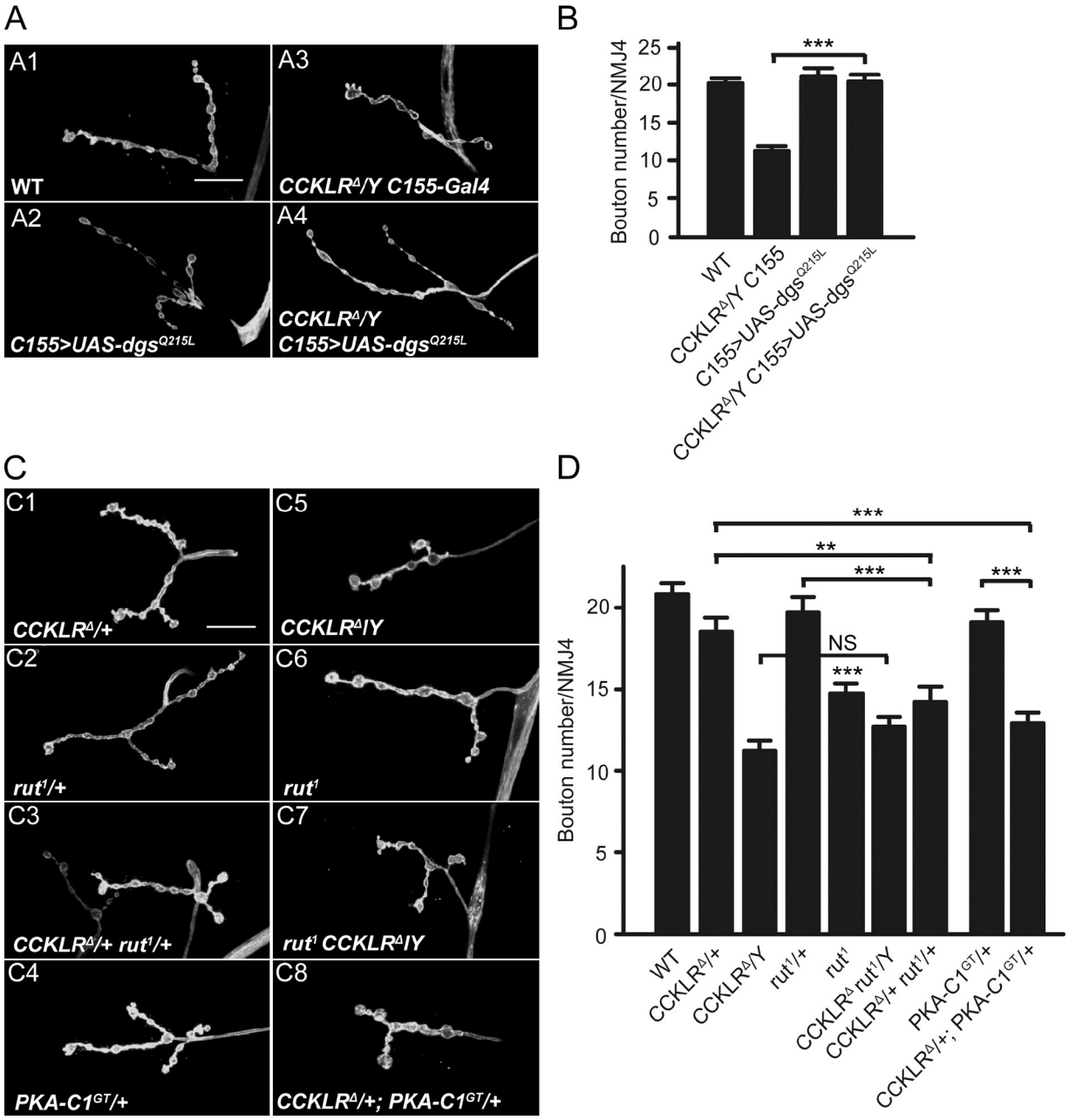

Figure 5. ***CCKLR* genetically interacts with components of the cAMP–PKA pathway.** (A and C) Confocal images of NMJ4 labeled with FITC–anti-HRP. (A) Overexpression of dgs^{Q215L}, a gain-of-function allele, suppresses NMJ undergrowth of $CCKLR^{\Delta}/Y$. (B) Quantification of bouton numbers at NMJ4 in larvae of the genotypes shown in A. (C) $rut^{1}/+$ $CCKLR^{\Delta}/+$ double heterozygotes (C3) show significantly enhanced undergrowth compared with either single heterozygote (C1 and C2). Similarly, $CCKLR^{\Delta}/+$; $PKA\text{-}C1^{GT}/+$ double heterozygotes (C8) exhibit significantly enhanced undergrowth compared with either single heterozygote (C1 and C4). rut^{1} homozygotes show NMJ undergrowth (C6). rut^{1} $CCKLR^{\Delta}$ double mutants (C7) do not show further undergrowth compared with $CCKLR^{\Delta}/Y$ (C5). Bars, 20 µm. (D) Quantification of bouton numbers at NMJ4 in larvae of the genotypes shown in C. $PKA\text{-}C1^{GT}$ is $PKA\text{-}C1^{BG02142}$. $C155{>}UAS\text{-}dgs^{Q215L}$ is $C155/Y$; $UAS\text{-}dgs^{Q215L}/+$. Error bars denote SEM. ***, $P < 0.001$; **, $P < 0.01$ (compared with WT control unless indicated otherwise).

CCKLR acts upstream of the cAMP pathway

When activated, GPCRs undergo a conformational change that allows the receptor to promote the exchange of GDP for GTP on the Gα subunit of heterotrimeric G proteins (McCudden et al., 2005). This exchange triggers the dissociation of the Gα subunit from the Gβγ dimer, and both Gα-GTP and Gβγ can then activate different second messenger pathways such as the cAMP signal pathway through stimulation of adenylyl cyclase (AC; Gilman, 1987; Neves et al., 2002). Previous studies have shown that a loss-of-function mutation in the gene encoding the stimulatory G protein α subunit (Gsα) in *Drosophila* (dgs^{M19}) causes NMJ undergrowth (Wolfgang et al., 2004). If *dgs* functions downstream of *CCKLR*, we hypothesized that overexpression of $UAS\text{-}dgs^{Q215L}$, a constitutively active Gsα construct (Renden and Broadie, 2003), could suppress the *CCKLR* mutant phenotype. When driven by *C155-Gal4*, overexpression of $UAS\text{-}dgs^{Q215L}$ in a WT background did not alter NMJ morphology

(Fig. 5, A2 and B). However, overexpression of *UAS-dgs*^{Q215L} completely suppresses the NMJ undergrowth phenotype of *CCKLR*$^{\Delta}$-null mutants (20.4 ± 0.9 vs. 11.2 ± 0.6 boutons; Fig. 5, A4 and B). Thus, NMJ undergrowth in *CCKLR* mutants appears to entail a decrease in signaling through Gsα.

A major signal transduction pathway downstream of GPCRs and stimulatory G proteins is the cAMP pathway via activation of AC, one of which is encoded by the *rutabaga* (*rut*) locus in *Drosophila* (Levin et al., 1992). Therefore, we examined *rut*^{1} mutations for their effect on NMJ growth and interaction with *CCKLR* mutations. As previously reported (Zhong et al., 1992), *rut*^{1} causes a mild undergrowth phenotype (Fig. 5, C6 and D). Heterozygous *rut*^{1}/+ (19.7 ± 0.9 boutons) and heterozygous *CCKLR*$^{\Delta}$/+ (18.5 ± 0.8 boutons) larvae have NMJs that do not differ from WT (Fig. 5, C1 and C2). However, heterozygosity for *rut*^{1} in a *CCKLR*$^{\Delta}$/+ background results in a significant reduction in NMJ growth (14.2 ± 0.9 boutons; Fig. 5, C3 and D), which suggests impairments in a common pathway. We generated a *rut*^{1} *CCKLR*$^{\Delta}$ double mutant by recombination and found that there was no further reduction in bouton number in double mutant homozygotes compared with *CCKLR*$^{\Delta}$ single mutants (Fig. 5, C7 and D). Collectively, these results point toward *CCKLR* and *rut* being involved in a common pathway.

Similarly, we found that the undergrowth phenotype of *CCKLR*$^{\Delta}$/+ heterozygotes is significantly enhanced by heterozygosity for *Df(2L)N22-14*, which uncovers *PKA-C1*, a cAMP-dependent protein kinase (data not shown), or for a mutation in this gene (*PKA-C1*^{BG02142}, referred to as *PKA-C1*^{GT}; 12.9 ± 0.6 boutons for *CCKLR*$^{\Delta}$/+; *PKA-C1*^{GT}/+ vs. 18.5 ± 0.8 boutons for *CCKLR*$^{\Delta}$/+ and 19.1 ± 0.7 boutons for *PKA-C1*^{GT}/+; Fig. 5, C8 and D). These results strongly support the idea that CCKLR regulates NMJ growth via activation of the cAMP pathway.

dCreb2 positively regulates NMJ growth and is epistatic to *CCKLR*

A major downstream regulator of the cAMP signaling pathway is CREB. Activation of CREB in response to elevated levels of cAMP leads to transcription of genes required for modifications in synaptic structure and function that are involved in long-term plasticity (Davis et al., 1996; Alberini, 2009). In *Drosophila*, although *dCreb2* has been shown to regulate activity-dependent functional plasticity at larval NMJs, its role in regulating NMJ growth during development has not been previously established (Davis et al., 1996; Koon et al., 2011). Having found that the cAMP pathway is required for CCKLR-dependent NMJ growth, we sought to determine if this phenotype is mediated through *dCreb2*. We observed a significant decrease in bouton number in *dCreb2* mutants *dCreb2*^{S162} and *dCreb2*^{EP}/*Df* (Fig. 6, A2 and B), which is comparable to that of *CCKLR* mutants. Similarly, overexpression of a dominant-negative (transcriptional blocker) *dCreb2* transgene (*UAS-Creb2.b*) in otherwise WT neurons also causes NMJ undergrowth (Fig. 6, A4 and B). In contrast, overexpression of *UAS-Creb2.a*, a WT form (transcriptional activator) of *dCreb2*, causes a mild but significant increase in bouton number (Fig. 6, A3 and B).

Loss of one copy of *dCreb2* in an otherwise WT background has no effect on NMJ morphology but significantly enhances NMJ undergrowth in *CCKLR*$^{\Delta}$/+ heterozygotes (14.3 ± 0.8 vs. 18.5 ± 0.8 boutons; Fig. 6, C3 and D). Remarkably, overexpression of *UAS-dCreb2.a* by *Elav-Gal4* not only fully suppresses the NMJ undergrowth of *CCKLR* mutants but even produces the same mild overgrowth phenotype as in a WT background (26.4 ± 1.0 vs. 13.2 ± 1.2 boutons; Fig. 6, C5 and D). In contrast, overexpression of *UAS-dCreb2.b* neither suppresses nor enhances *CCKLR* phenotypes (15.4 ± 0.8 vs. 13.2 ± 1.2 boutons; Fig. 6, C6 and D). These results demonstrate that in addition to its previously described role in functional synaptic plasticity (Davis et al., 1996), dCREB2 strongly regulates NMJ growth during development and is a major downstream target through which CCKLR promotes NMJ growth.

Presynaptic overexpression of *CCKLR* leads to NMJ overgrowth

Our results thus far indicate that CCKLR is a positive regulator of NMJ growth. If the CCKLR pathway does stimulate NMJ growth, enhancement of the activity of this pathway could lead to NMJ overgrowth. To investigate this possibility, we overexpressed the *UAS-CCKLR* transgene in an otherwise WT background. Overexpression of a single copy of *UAS-CCKLR* either in neurons (*Elav-Gal4*) or in muscles (*24B-Gal4*) has no effect on NMJ morphology (unpublished data). However, when two copies of *UAS-CCKLR* are driven by *Elav-Gal4* (*Gal4/+; UAS/UAS*, designated as *Gal4>2X*(*UAS*)), there is a significant increase in bouton number (28.9 ± 1.0 vs. 19.4 ± 1.5; Fig. 7, A2 and B). This overgrowth phenotype is very similar to that caused by overexpression of *UAS-Creb2.a* (Fig. 6, A3 and B). To avoid possible genetic background effects associated with homozygosity for *UAS-CCKLR*, we repeated the 2X(*UAS-CCKLR*) neuronal overexpression using a heterozygous combination of two independent *UAS-CCKLR* transgenes and observed the same overgrowth phenotype (unpublished data). In contrast, overexpression of two copies of *UAS-CCKLR* in muscle still had no effect on NMJ morphology (Fig. 7, A3 and B). These results provide additional support for the conclusion that CCKLR functions presynaptically as a positive regulator of NMJ growth.

We also examined overexpression of 2X(*UAS-dsk*) in either neurons or muscles in an otherwise WT background. In neither instance did we observe a significant effect on NMJ morphology (Fig. 7, A5, A6, and B). Thus, increasing the level of *dsk* expression in WT larvae does not perturb NMJ growth, which suggests that it is the endogenous receptor rather than the neuropeptide ligand that is normally present in limiting amounts.

DSK/CCKLR signaling is required for normal synaptic function

Although both *CCKLR* and *dsk* mutants have reductions in bouton number, the mutant boutons appear generally larger than WT (especially in *CCKLR*$^{\Delta}$/*Y* larvae), raising the question of whether there could be some type of structural compensation for the deficit in bouton number. One way the NMJ could compensate for having fewer boutons would be to increase the density of

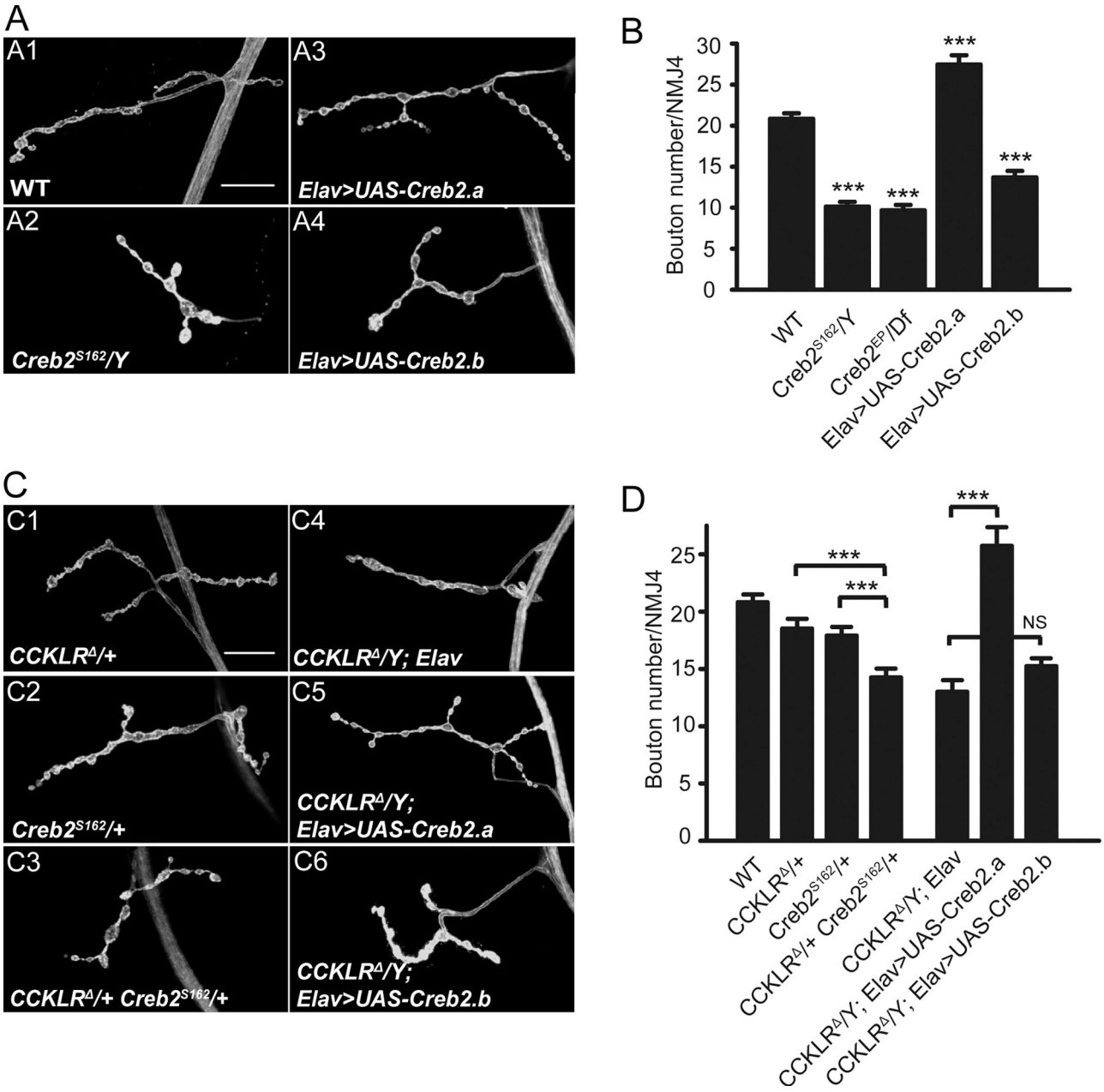

Figure 6. ***dCreb2* positively regulates NMJ growth and is epistatic to *CCKLR*.** (A and C) Confocal images of NMJ4 labeled with FITC–anti-HRP. (A) *Creb2*^{S162} hemizygotes exhibit strong NMJ undergrowth similar to *CCKLR*$^{\Delta}$*/Y* (A2). Neuronal overexpression of *Creb2.a* by *Elav-Gal4* (*Elav>UAS-Creb2.a*) results in NMJ overgrowth (A3), whereas neuronal overexpression of *Creb2.b* (*Elav>UAS-Creb2.b*) leads to NMJ undergrowth (A4). (B) Quantification of bouton numbers at NMJ4 in *Creb2* mutant larvae and larvae with *Creb2* misexpression. *Creb*^{EP}*/Df* is *Creb*^{EP1378}*/Df (1)os*^{UE69}. (C) Genetic interactions between *CCKLR* and *Creb2*. *Creb2*^{S162}*/+ CCKLR*$^{\Delta}$*/+* double heterozygotes (C3) exhibit significantly enhanced NMJ undergrowth compared with either single heterozygote (C1 and C2). Neuronal overexpression of *Creb2.a* suppresses NMJ undergrowth of *CCKLR*$^{\Delta}$*/Y* and leads to overgrowth (C5), whereas overexpression of *Creb2.b* does not (C6). Bars, 20 µm. (D) Quantification of bouton numbers at NMJ4 in larvae of the genotypes shown in C. Error bars denote SEM. ***, P < 0.001 (compared with WT control unless indicated otherwise). *Elav>UAS-Creb2.a* or *-b* is *Elav-Gal4/UAS-Creb2.a* or *-b*.

active zones within the remaining boutons. To determine if there was any effect on the number or distribution of active zones, we stained with anti-Bruchpilot (anti-Brp) and anti-GluRIIC antibodies to label both pre- and postsynaptic components. The number of active zones per bouton is slightly higher in *CCKLR*$^{\Delta}$*/Y* mutants compared with WT, but this difference is not significant (Fig. 8, A and B). Similarly, the number of active zones per bouton is normal in *dsk* mutants (Fig. 8, A and B). Thus, as a result of the reduction in bouton number, the total number of active zones per NMJ is significantly reduced in both *CCKLR* (209 ± 11) and *dsk* mutants (180 ± 12) compared with WT (308 ± 15; Fig. 8 C). The apposition of pre- and postsynaptic active zones, stained with anti-Brp and anti-GluRIIC antibodies, respectively, appear normal in both *dsk* and *CCKLR* mutants, as do the levels of these proteins (Fig. 8 A). Similarly, the levels of GluRIIB in the mutants do not differ from control larvae (Fig. S4).

To determine if the reduction in active zone number is associated with a reduction in synaptic transmission, we recorded

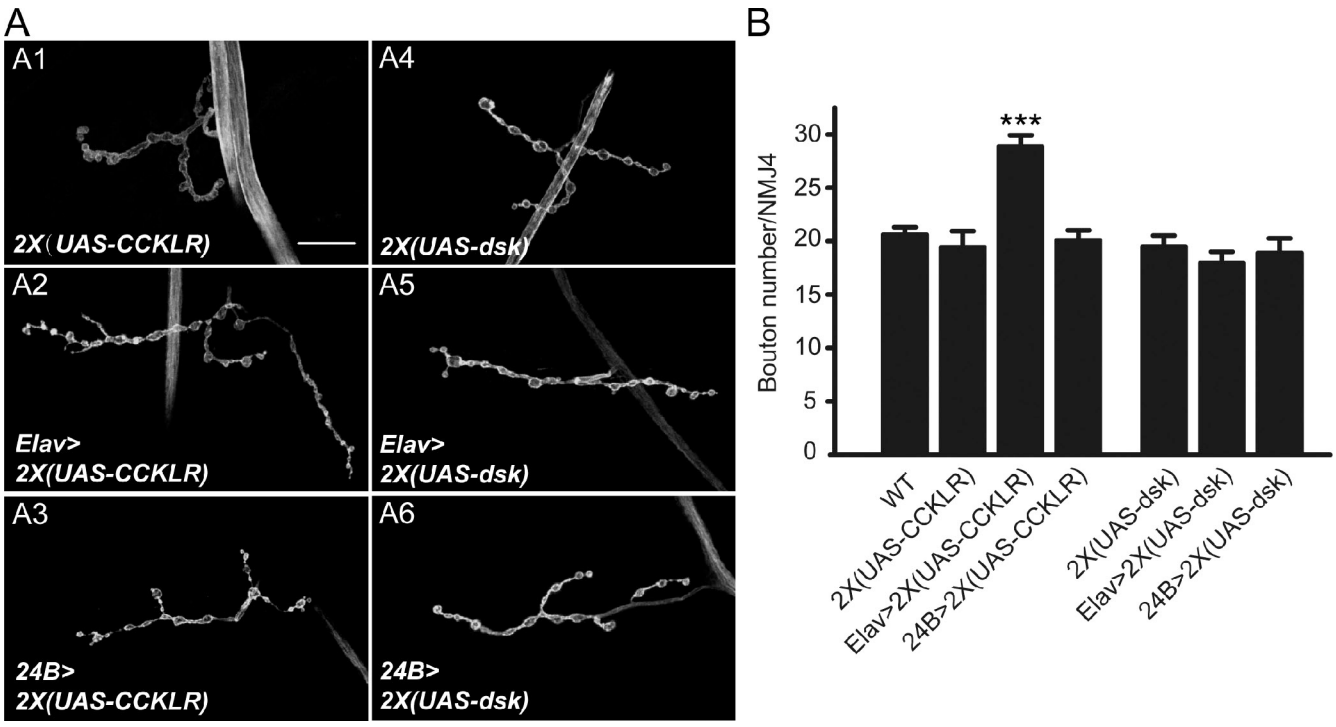

Figure 7. **Presynaptic overexpression of *CCKLR* leads to NMJ overgrowth.** (A) Confocal images of NMJ4 labeled with FITC–anti-HRP. Neuronal overexpression of two copies of *CCKLR* by *Elav-Gal4* (*Elav*>2X(*UAS-CCKLR*)) results in a significant increase in NMJ growth (A2). Overexpression in muscle (*24B*>2X(*UAS-CCKLR*)) does not alter NMJ growth (A3). Overexpression of 2X(*UAS-dsk*) by either *Elav-Gal4* (A5) or *24B-Gal4* (A6) does not affect NMJ growth. Bar, 20 µm. (B) Quantification of bouton numbers at NMJ4 in larvae of the genotypes shown in A. The genotype of *Gal4>2X(UAS) is Gal4/+; UAS /UAS*. Error bars denote SEM. ***, $P < 0.001$ (compared with WT control).

excitatory junction potentials (EJPs) from muscle 6. We did not detect any significant difference in the size or frequency of miniature EJPs (mEJPs) in *CCKLR* or *dsk* mutants compared with WT controls (Fig. 9, A–C). However, the size of EJPs in both *CCKLR* (12.12 ± 1.71 mV) and *dsk* mutants (11.78 ± 1.13 mV) is reduced by 50% compared with controls (23.73 ± 2.90 mV; Fig. 9, D and E). Thus, there is a significant reduction in the quantal content (number of vesicles released per stimulus) in *CCKLR* (27.15 ± 2.90) and *dsk* mutants (21.68 ± 2.44) compared with WT (55.98 ± 6.19) that parallels their decrease in number of active zones (Fig. 9 F). The EJP defect in *CCKLR* and *dsk* mutants is substantially rescued by expressing a *UAS-CCKLR* transgene under the direction of *C155-Gal4* or by introducing a WT copy of *dsk* via a chromosome duplication (Fig. 9 E), which is similar to what we previously found for bouton number. Thus, *CCKLR* and *dsk* mutants have deficits in synaptic transmission, and there is very good correlation between the reduction in number of active zones and the reduction in EJP amplitude. Nonetheless, it is important to note that the CCKLR–cAMP–CREB signaling pathway could still be affecting transmitter release via a mechanism that is distinct from its effects on NMJ morphology.

Discussion

Using an unbiased, forward genetic approach, we discovered that CCKLR, a GPCR, together with its presumptive ligand, DSK, are positive regulators of NMJ growth in *Drosophila*. In addition, we demonstrate that DSK/CCKLR mediates NMJ development via the cAMP–PKA–CREB pathway, which is also required for learning and memory. These findings reveal a novel role for neuropeptide signaling in synaptic development and suggest a possible mechanistic link between pathways regulating synaptic growth and those regulating long-term synaptic plasticity.

A role for DSK/CCKLR signaling in NMJ growth regulation

Neuropeptides, whose effects have been extensively studied at NMJs, are usually described as neuromodulators because they modify the strength of synaptic transmission. For example, proctolin can potentiate the action of glutamate at certain NMJs in insects (Adams and O'Shea, 1983). However, involvement of neuropeptides in regulating neural development has not been well characterized. Recently, a C-type natriuretic peptide acting through a cGMP signaling cascade was found to be required for sensory axon bifurcation in mice (Schmidt et al., 2009), which suggests that neuropeptides may have a broader role in development than previously appreciated. Our studies demonstrate that DSK and its receptor, CCKLR, are strong positive regulators of NMJ growth in *Drosophila*.

DSK belongs to the family of FMRFamide-related peptides (FaRPs), which is very broadly distributed across invertebrate and vertebrate phyla. Originally identified in clams (Price and Greenberg, 1977), FaRPs affect heart rate, blood pressure, gut motility, feeding behavior, and reproduction in invertebrates

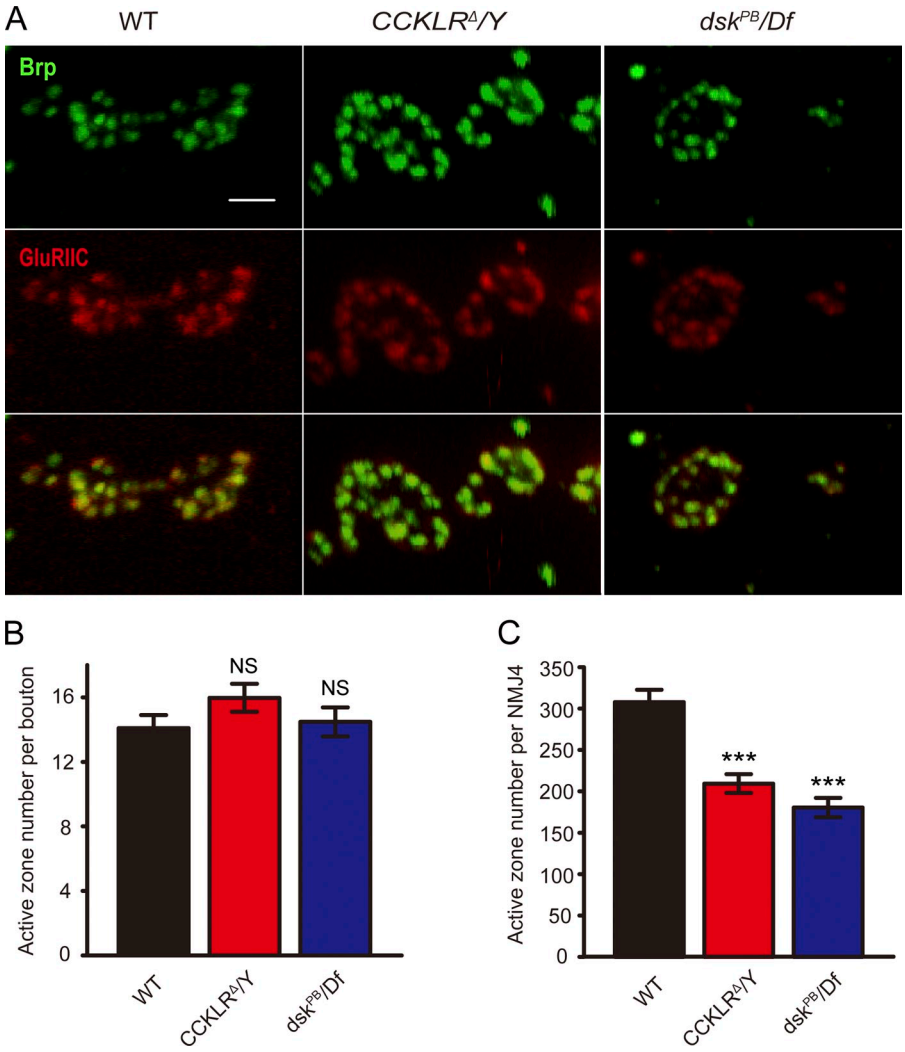

Figure 8. **Active zone density per bouton is normal in *CCKLR* and *dsk* mutants but the total number per NMJ is reduced.** (A) Confocal images of NMJ4 boutons labeled with anti-Brp (green) and anti-GluRIIC (red). Bar, 2 µm. (B) Quantification of active zones per bouton for larvae of the indicated genotypes. (C) Quantification of total active zones per NMJ4 for larvae of the indicated genotypes (WT, n = 10; $CCKLR^{\Delta}/Y$, n = 10; dsk^{PB}/Df, n = 12. n is the number of NMJs scored). Error bars denote SEM. ***, P < 0.001(compared with WT control). NS, not significant compared with WT control.

(Li et al., 1999; Nichols, 2006; Audsley and Weaver, 2009). They have been shown to enhance synaptic efficacy at NMJs in locust and to modulate presynaptic Ca^{2+} channel activity in crustaceans (Robb and Evans, 1994; Rathmayer et al., 2002). In *Drosophila*, various neuropeptides derived from the *FMRFa* gene can modulate the strength of muscle contraction when perfused onto standard larval nerve–muscle preparations (Hewes et al., 1998). To these previously described functions of FaRPs, we now add a new role as a positive regulator of NMJ development.

DSK/CCKLR signals through the cAMP–PKA–CREB pathway to regulate NMJ development

Transgenic rescue experiments, RNAi expression, and overexpression of WT *CCKLR* demonstrate that CCKLR functions presynaptically in motor neurons to promote NMJ growth. Downstream components of this pathway were identified on the basis of known biochemistry of GPCRs and phenotypic interactions in double mutant combinations. GPCRs typically function by activating second messenger pathways via G proteins. Because loss-of-function mutations in *dgs*, which encodes the Gsα subunit in *Drosophila*, cause NMJ undergrowth (Wolfgang et al., 2004), we hypothesized that CCKLR signals through Gsα. Consistent with this idea, we found that presynaptic constitutively active *dgs* overexpression rescues the NMJ undergrowth phenotype of *CCKLR* mutants. Conversely, we observe dominant dose-dependent interactions between *CCKLR*-null mutations and mutations of *rut*, which encodes an AC; or *PKA-C1*, which encodes a cAMP-dependent protein kinase, resulting in significant reductions in NMJ growth. These data place *CCKLR* together with the other genes in a common cAMP-dependent signaling pathway that regulates NMJ growth.

It is known that the AC encoded by *rut* is activated by Gsα, and on the basis of our results, we propose that it is downstream of CCKLR signaling. However, the NMJ undergrowth in rut^1, which is a presumptive null mutant, is not as severe as that of a *CCKLR*-null mutant. This is likely due to the fact that the *Drosophila* genome contains up to seven different AC-encoding genes, all of which are stimulated by Gsα (Cann and Levin, 1998). Presumably, one or more additional AC-encoding genes share some functional overlap with *rut* in regulation of NMJ growth. This idea is in good agreement with the results of Wolfgang et al., (2004), who found that the NMJ undergrowth phenotype of rut^1 is weaker

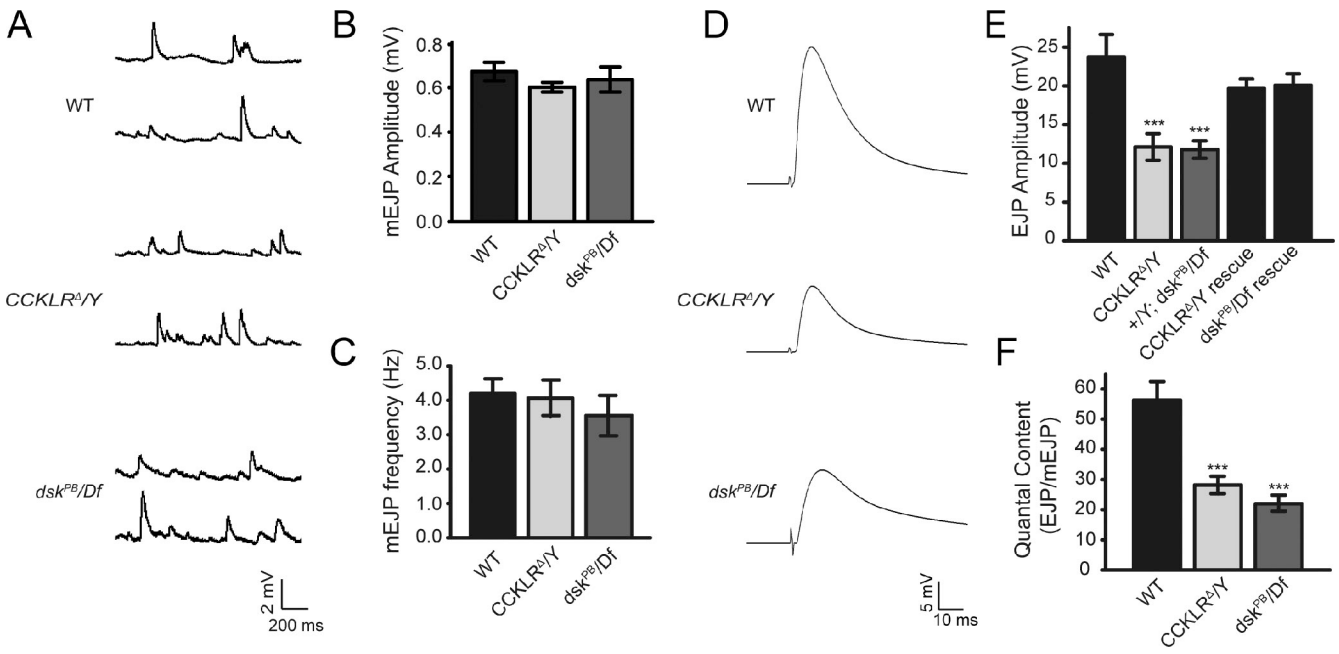

Figure 9. ***CCKLR* and *dsk* mutants exhibit a reduction in evoked neurotransmission.** (A) Representative traces of spontaneous neurotransmitter release recorded in 0.5 mM Ca^{2+} from muscle 6 in third instar larvae of the indicated genotypes. (B and C) Quantification of the mean mEJP amplitude and frequency of WT (n = 12), *CCKLR*$^{\Delta}$*/Y* (n = 12), and *dsk* ^{PB}*/Df* (n = 11). (D) Representative traces of evoked transmitter release recorded in 0.5 mM Ca^{2+} from muscle 6. (E) Quantification of the mean EJP amplitude. The mean EJP amplitude is significantly reduced in *CCKLR*$^{\Delta}$*/Y* (n = 10) and *dsk*^{PB}*/Df* (n = 9) mutants compared with WT (n = 7; P < 0.001). *C155-Gal4*–driven *UAS-CCKLR* expression (n = 15) and the Dp carrying dsk^{+} (n = 11) rescue the defects of *CCKLR*$^{\Delta}$*/Y* and *dsk*^{PB}*/Df*, respectively. (F) Quantal content is significantly reduced in *CCKLR*$^{\Delta}$*/Y* (n = 12) and *dsk*^{PB}*/Df* (n = 11) mutants (P < 0.001). Mean quantal content was determined for each recording by dividing the mean super-threshold EJP amplitude by the mean mEJP amplitude. EJP amplitudes were corrected for nonlinear summation before calculation of quantal content. Error bars denote SEM. ***, P < 0.001(compared with WT control).

than that of *dgs* mutants, which they also interpreted as an indication that multiple ACs are activated by the Gsα encoded by *dgs*.

The primary effector of this pathway is CREB2, a transcriptional regulatory protein that is activated upon phosphorylation by PKA. Consistent with the idea that CCKLR ultimately acts via activation of CREB, loss-of-function mutations of *dCreb2* or neuronal overexpression of a dominant-negative *dCreb2* transgene cause NMJ undergrowth similar to that of *CCKLR*-null mutants. Additionally, loss of one copy of *dCreb2* in a *CCKLR* heterozygous background also causes NMJ undergrowth, and overexpression of WT *dCreb2* fully rescues the NMJ undergrowth phenotype of *CCKLR* null, even leading to NMJ overgrowth. Thus, regulation of NMJ growth through the CCKLR signaling pathway is clearly mediated by *dCreb2*, whose activity is itself necessary and sufficient for regulating NMJ growth. This conclusion differs from Davis et al. (1996), who suggested that *dCreb2* is required for NMJ function but not NMJ growth. One possible explanation for this discrepancy is that a weaker, inducible heat shock–driven transgene was used to express *dCreb2* in the earlier work, whereas strong constitutive neuronal drivers were used here. In any case, our results demonstrate that in addition to its known role in NMJ function (Davis et al., 1996), CREB2 is also a strong positive regulator of NMJ growth and is likely to play a greater role in structural plasticity of synapses in learning and memory in *Drosophila* than previously suggested. This conclusion is consistent with a recent study indicating that sprouting of type II larval NMJs in response to starvation is stimulated by a cAMP/CREB-dependent pathway via activation of an octopamine GPCR (Koon et al., 2011).

DSK/CCKLR signaling is required for normal synaptic function

In addition to being undergrown, NMJs in *CCKLR* mutant larvae also exhibit a functional deficit. This is perhaps less straightforward than it might seem. Previous analyses of mutations affecting growth of the larval NMJ in *Drosophila* have shown that there is no simple correlation between the size and complexity of the NMJ and the amplitude of EJPs or amount of neurotransmitter release. These discrepancies arise because of various homeostatic compensatory mechanisms and because some of the affected signaling pathways alter synaptic growth and synaptic function in different ways via distinct downstream targets. For example, a mutation in *highwire*, which has the most extreme NMJ overgrowth phenotype described, is associated with a decrease in synaptic transmission (Wan et al., 2000). *Wallenda* mutations have been shown to fully suppress the overgrowth phenotype, but have no effect on the deficit in synaptic transmission (Collins et al., 2006).

In the case of *CCKLR* mutants, however, there appears to be a very good correspondence between the morphological phenotype and the electrophysiological phenotype: the reduction in the total number of active zones in *CCKLR* larvae as measured morphologically correlates very well with the reduction in quantal content we observe. In addition, we did not

detect any difference in *CCKLR* mutants in calcium sensitivity of transmitter release or in the size or frequency of spontaneous release events. Thus, the synaptic growth phenotype of *CCKLR* mutant NMJs is sufficient to account for the functional phenotype. However, we cannot rule out the possibility that DSK/CCKLR signaling also exerts some modulatory effect on NMJ function that is distinct from its effect on NMJ development.

DSK as the CCKLR ligand

DSK is identified as the *Drosophila* orthologue of CCK, the ligand of CCKLR in vertebrates, on the basis of sequence analysis. Our genetic analysis strongly supports the conclusion that DSK is the ligand of CCKLR at the larval NMJ. First, mutations of *dsk* and expression of *dsk* RNAi result in NMJ undergrowth phenotypes similar to that of *CCKLR* mutants. Second, loss of one copy of both *dsk* and *CCKLR* in double heterozygotes results in NMJ undergrowth. Third, heterozygosity for *dsk* does not further enhance the phenotype of a *CCKLR*-null mutant as expected if DSK regulates NMJ growth through its action on CCKLR. Fourth, overexpression of *UAS-dsk* does not rescue the undergrowth phenotype of a *CCKLR*-null mutant, but *CCKLR* overexpression can rescue NMJ undergrowth of a *dsk* hypomorphic mutant.

The discovery of an entirely novel role for neuropeptide signaling in NMJ growth raises several questions about how this signaling is regulated and the biological significance of this mechanism. Although answers to these questions will require much additional work, an immediate question is whether a paracrine or autocrine mechanism is involved. In the case of octopamine-mediated synaptic sprouting in response to starvation, both autocrine and paracrine signaling are involved in the sprouting of type II and type I NMJs, respectively (Koon et al., 2011). In an early immunohistochemical investigation, Nichols (1992) reported that DSK was detected in medial neurosecretory cells in the larval CNS that extended projections anteriorly into the brain and posteriorly to the ventral ganglion (Nichols, 1992). As we were unable to obtain the original DSK antiserum and were unsuccessful in raising our own antiserum, we have not been able to confirm or extend the previous report. Instead, we performed tissue-specific RNAi experiments to examine the spatial requirement for DSK. Pan-neuronal *dsk* RNAi expression indicates that DSK expression in neurons is required to promote NMJ growth. In addition, *C739-Gal4*–driven *dsk* RNAi also causes NMJ undergrowth, whereas *OK-Gal4*–driven *dsk* RNAi in motor neurons does not. The expression pattern of *C739-Gal4* overlaps with the DSK-positive cells previously identified by immunohistochemistry, which suggests that DSK produced by those neurosecretory cells is required for normal NMJ growth. Thus, from available data, it seems most likely that DSK is acting in paracrine fashion to regulate NMJ growth. However, further investigation will be necessary to determine the exact source of the DSK that promotes NMJ growth to fully understand how this neuropeptide regulates NMJ development.

Linking synaptic growth and synaptic plasticity

Studies have demonstrated a role for CREB in long-term synaptic plasticity—structural changes in synaptic morphology that underlie the formation of long-term memories (Benito and Barco, 2010). Here we show that in addition to CREB's role in structural modification of synapses in response to experience after development is complete, it is also a key regulator of growth and morphology during development of the larval NMJ. Moreover, although CREB is the transcriptional effector for many GPCRs, the fact that NMJs in *CCKLR* mutants are as undergrown as those of CREB mutants suggests that DSK/CCKLR signaling is a major input to CREB during NMJ growth. Many of the genes encoding intermediate components of the pathway such as *dnc*, *rut*, and *PKA* also have effects on NMJ growth and development as well as on synaptic plasticity and learning and memory, further emphasizing an overlap between the mechanisms that regulate synaptic growth during development and those that regulate postdevelopmental structural synaptic plasticity. These results raise the possibility that DSK/CCKLR signaling also plays a role in long-term synaptic plasticity and learning as well as in synaptic development.

Materials and methods

Fly stocks

w^{1118} was used as WT control for genetic background. *B185-Gal4* was provided by G. Davis (University of California, San Francisco, San Francisco, CA). rut^{1} was provided by C.F. Wu (University of Iowa, Iowa City, IA). *UAS-Creb2.b* was provided by J. Yin (University of Wisconsin-Madison, Madison, WI). *C155-Gal4 UAS-Dcr* was provided by K. O'Connor-Giles (University of Wisconsin-Madison). The following fly lines were obtained from the Bloomington Stock Center: *Df(1)fu-A7*, *Df(1)Exel9051*, *Df(1)ED7413*, *Dp(1;3)DC351*, *Dp(1;3) DC352*, *Dp(3;1)2-2*, *Df(3R)2-2*, $Df(1)os^{UE69}$, *Df(2L)N22-14*, $CCKLR^{MB02688}$, *CCKLR-17D3*^{KG01373}, *C155-Gal4*, *Elav-Gal4*, *24B-Gal4*, *OK6-Gal4*, *C739-Gal4*, dsk^{EP3632}, $UAS\text{-}dgs^{Q215L}$, $PKA\text{-}C1^{BG02142}$, $dCreb2^{S162}$, $dCreb2^{EP1378}$, and *UAS-Creb2.a* (Perazzona et al., 2004). *UAS-CCKLR-RNAi* (no. 7231) and *UAS-dsk-RNAi* (no. 14201) were obtained from the Vienna Drosophila RNAi Center. dsk^{f02468} was obtained from the Exelixis collection at Harvard Medical School. $CCKLR^{\Delta}$ *C155-Gal4* was derived by recombination between *Df(1)Exel9051* and *C155-Gal4* and confirmed by PCR for the *CCKLR* deletion and *C155-Gal4*–driven *UAS-CD8–GFP* expression pattern. rut^{1} $CCKLR^{\Delta}$ was built by recombination between *Df(1)Exel9051* and rut^{1} and confirmed by PCR for the *CCKLR* deletion and sequencing for the rut^{1} lesion. All stocks were raised on cornmeal/molasses fly medium and maintained at RT (21–23°C).

Immunohistochemistry

Wandering third instar larvae were dissected in Ca^{2+}-free ice-cold saline and fixed in 4% paraformaldehyde for 20 min. Larvae were incubated in primary antibodies overnight at 4°C or for 2–3 h at room temperature and in secondary antibodies for 1–2 h at room temperature, then mounted in VectaShield (Vector Laboratories) for microscopic analysis. We used the following antibodies: FITC-conjugated or Cy5-conjugeted anti-HRP at 1:100 (Jackson ImmunoResearch Laboratories, Inc.), mouse anti-Elav at 1:500 (Developmental Studies Hybridoma Bank), mouse anti-Brp (nc82) at 1:50 (Developmental Studies Hybridoma Bank), rabbit anti-GluRIIB, and rabbit anti-GluRIIC (DiAntonio laboratory, Washington University, St. Louis, MO). To detect CCKLR–mCherry fusion protein, rabbit anti-DsRed (Takara Bio Inc.) was used at 1:500. Specific secondary antibodies conjugated to Alexa Fluor 488, Alexa Fluor 568, and Alexa Fluor 633 (Invitrogen) were used at 1:200.

Imaging and quantification

Although we concentrated on NMJ4 because of its relative simplicity, we also observed comparable results at NMJ6/7 as well as other NMJs in the mutant larvae. Quantification of bouton number was performed at NMJ4 (Ib) in segments A2–A4. Boutons were scored by counting each distinct spherical anti-HRP stained varicosity along motor terminals. Bouton numbers for each genotype are summarized in Table S1. The muscle size of all larvae examined was similar. Corresponding controls were processed and quantified simultaneously with samples for each experiment. Statistical analyses were performed via analysis of variance and Student's *t* tests for multiple

comparisons. Significance levels of <0.05, <0.01, or <0.001 are indicated by one, two, and three asterisks, respectively. Error bars denote SEM. Confocal images were obtained on a microscope (LSM 510; Carl Zeiss) with Plan-Apochromat 20× NA 10.8 and EC Plan-Neofluar 40× NA 1.3 oil objective lenses and the accompanying software. Images were processed in the LSM image browser (Carl Zeiss). Brightness and contrast were adjusted using Photoshop (Adobe). All images were captured at room temperature (21–23°C).

Molecular cloning

UAS-CCKLR comprises a full-length *CCKLR* cDNA cloned into *pUAST*. Full-length cDNA was obtained by PCR amplification using *pOT2-IP18747* full insert cDNA clone (731–2,022 bp; Berkeley Drosophila Genome Project) and genomic DNA of WT flies (1–730 bp), and ligation of the two fragments. *UAS-CCKLR–mCherry* was generated by cloning *CCKLR* cDNA into the *pUAS-C5 attB-C-term mCherry* vector. *UAS-dsk* comprises a full-length *dsk* cDNA cloned into *pUAST-attB*. cDNA constructs for *dsk* were generated by amplification of the coding sequence using genomic DNA of WT flies. After germline transformation, *UAS-CCKLR*, *UAS-CCKLR–mCherry*, and *UAS-dsk* were inserted on chromosome 2 in a w^{1118} background, respectively. Primers flanking the predicted open reading frames incorporated restriction sites to facilitate directional cloning into the *pUAST* or *pUAST-attB* vector. The sequences of primers used are provided in Table S2. All receptor constructs were fully sequenced.

Electrophysiology

Intracellular recordings were performed at RT on muscle 6 (segments A2 or A3) or wandering third instar larvae as described previously (Petersen et al., 1997). Larvae were dissected in physiological saline HL-3 (Stewart et al., 1994) containing 0.5 mM Ca^{2+}. Data were considered valid when the resting membrane potential was between −60 and −80 mV, and the input resistance of the muscle was >5 MΩ. The mEJP amplitudes were measured by hand using the cursor option in Clampfit software (Axon Instrument), and mean mEJP amplitudes were calculated from mEJPs. Mean EJP size was calculated by measuring the amplitude of the computer-generated trace average of 50 consecutive EJP traces. Quantal content was estimated by dividing the mean EJP by the mean mEJP, and corrected for nonlinear summation according to Martin (1955).

Online supplemental material

Fig. S1 shows that *CCKLR-17D3* does not interact with *CCKLR-17D1* and does not affect NMJ growth. Fig. S2 shows that *CCKLR–mCherry* rescues $CCKLR^{\Delta}/Y$ and localizes to motor neurons. Fig. S3 shows that the *C739-Gal4* expression pattern overlaps with the previously reported DSK antiserum staining pattern. Fig. S4 shows that GluRIIB staining appears normal in $CCKLR^{\Delta}/Y$ and dsk^{PB}/Df larvae. Table S1 presents quantification of bouton numbers for each genotype. Table S2 presents sequences of primers used in constructs. Online supplemental material is available at http://www.jcb.org/cgi/content/full/jcb.201109044/DC1.

We are grateful to Chun-Fang Wu, Jerry Yin, Graeme Davis, Kate O'Connor-Giles, the Bloomington Stock Center, and the Vienna Drosophila RNAi Center for providing fly stocks used in these experiments. We thank all members of the Ganetzky laboratory, Kate O'Connor-Giles, and Grace Boekhoff-Falk for helpful discussion and critical comments on the manuscript.

This research was supported by a grant from the National Institutes of Health (NS15390) to B. Ganetzky.

Submitted: 8 September 2011
Accepted: 18 January 2012

References

Adams, M.E., and M. O'Shea. 1983. Peptide cotransmitter at a neuromuscular junction. *Science*. 221:286–289. http://dx.doi.org/10.1126/science.6134339

Alberini, C.M. 2009. Transcription factors in long-term memory and synaptic plasticity. *Physiol. Rev.* 89:121–145. http://dx.doi.org/10.1152/physrev.00017.2008

Audsley, N., and R.J. Weaver. 2009. Neuropeptides associated with the regulation of feeding in insects. *Gen. Comp. Endocrinol.* 162:93–104. http://dx.doi.org/10.1016/j.ygcen.2008.08.003

Benito, E., and A. Barco. 2010. CREB's control of intrinsic and synaptic plasticity: implications for CREB-dependent memory models. *Trends Neurosci.* 33:230–240. http://dx.doi.org/10.1016/j.tins.2010.02.001

Cann, M.J., and L.R. Levin. 1998. Genetic characterization of adenylyl cyclase function. *Adv. Second Messenger Phosphoprotein Res.* 32:121–135.

Collins, C.A., and A. DiAntonio. 2007. Synaptic development: insights from *Drosophila*. *Curr. Opin. Neurobiol.* 17:35–42. http://dx.doi.org/10.1016/j.conb.2007.01.001

Collins, C.A., Y.P. Wairkar, S.L. Johnson, and A. DiAntonio. 2006. Highwire restrains synaptic growth by attenuating a MAP kinase signal. *Neuron*. 51:57–69. http://dx.doi.org/10.1016/j.neuron.2006.05.026

Davis, G.W., C.M. Schuster, and C.S. Goodman. 1996. Genetic dissection of structural and functional components of synaptic plasticity. III. CREB is necessary for presynaptic functional plasticity. *Neuron*. 17:669–679. http://dx.doi.org/10.1016/S0896-6273(00)80199-3

Davis, G.W., C.M. Schuster, and C.S. Goodman. 1997. Genetic analysis of the mechanisms controlling target selection: target-derived Fasciclin II regulates the pattern of synapse formation. *Neuron*. 19:561–573. http://dx.doi.org/10.1016/S0896-6273(00)80372-4

Featherstone, D.E., and K. Broadie. 2000. Surprises from *Drosophila*: genetic mechanisms of synaptic development and plasticity. *Brain Res. Bull.* 53:501–511. http://dx.doi.org/10.1016/S0361-9230(00)00383-X

Gilman, A.G. 1987. G proteins: transducers of receptor-generated signals. *Annu. Rev. Biochem.* 56:615–649. http://dx.doi.org/10.1146/annurev.bi.56.070187.003151

Hewes, R.S., E.C. Snowdeal III, M. Saitoe, and P.H. Taghert. 1998. Functional redundancy of FMRFamide-related peptides at the *Drosophila* larval neuromuscular junction. *J. Neurosci.* 18:7138–7151.

Koon, A.C., J. Ashley, R. Barria, S. DasGupta, R. Brain, S. Waddell, M.J. Alkema, and V. Budnik. 2011. Autoregulatory and paracrine control of synaptic and behavioral plasticity by octopaminergic signaling. *Nat. Neurosci.* 14:190–199. http://dx.doi.org/10.1038/nn.2716

Levin, L.R., P.L. Han, P.M. Hwang, P.G. Feinstein, R.L. Davis, and R.R. Reed. 1992. The *Drosophila* learning and memory gene rutabaga encodes a Ca2+/Calmodulin-responsive adenylyl cyclase. *Cell*. 68:479–489. http://dx.doi.org/10.1016/0092-8674(92)90185-F

Li, C., K. Kim, and L.S. Nelson. 1999. FMRFamide-related neuropeptide gene family in *Caenorhabditis elegans*. *Brain Res.* 848:26–34. http://dx.doi.org/10.1016/S0006-8993(99)01972-1

Manseau, L., A. Baradaran, D. Brower, A. Budhu, F. Elefant, H. Phan, A.V. Philp, M. Yang, D. Glover, K. Kaiser, et al. 1997. GAL4 enhancer traps expressed in the embryo, larval brain, imaginal discs, and ovary of *Drosophila*. *Dev. Dyn.* 209:310–322. http://dx.doi.org/10.1002/(SICI)1097-0177(199707)209:3<310::AID-AJA6>3.0.CO;2-L

Martin, A.R. 1955. A further study of the statistical composition on the end-plate potential. *J. Physiol.* 130:114–122.

McCudden, C.R., M.D. Hains, R.J. Kimple, D.P. Siderovski, and F.S. Willard. 2005. G-protein signaling: back to the future. *Cell. Mol. Life Sci.* 62:551–577. http://dx.doi.org/10.1007/s00018-004-4462-3

Nässel, D.R. 2002. Neuropeptides in the nervous system of *Drosophila* and other insects: multiple roles as neuromodulators and neurohormones. *Prog. Neurobiol.* 68:1–84. http://dx.doi.org/10.1016/S0301-0082(02)00057-6

Nässel, D.R., and A.M. Winther. 2010. *Drosophila* neuropeptides in regulation of physiology and behavior. *Prog. Neurobiol.* 92:42–104. http://dx.doi.org/10.1016/j.pneurobio.2010.04.010

Neves, S.R., P.T. Ram, and R. Iyengar. 2002. G protein pathways. *Science*. 296:1636–1639. http://dx.doi.org/10.1126/science.1071550

Nichols, R. 1992. Isolation and expression of the *Drosophila* drosulfakinin neural peptide gene product, DSK-I. *Mol. Cell. Neurosci.* 3:342–347. http://dx.doi.org/10.1016/1044-7431(92)90031-V

Nichols, R. 2003. Signaling pathways and physiological functions of *Drosophila melanogaster* FMRFamide-related peptides. *Annu. Rev. Entomol.* 48:485–503. http://dx.doi.org/10.1146/annurev.ento.48.091801.112525

Nichols, R. 2006. FMRFamide-related peptides and serotonin regulate *Drosophila melanogaster* heart rate: mechanisms and structure requirements. *Peptides*. 27:1130–1137. http://dx.doi.org/10.1016/j.peptides.2005.07.032

Perazzona, B., G. Isabel, T. Preat, and R.L. Davis. 2004. The role of cAMP response element-binding protein in *Drosophila* long-term memory. *J. Neurosci.* 24:8823–8828. http://dx.doi.org/10.1523/JNEUROSCI.4542-03.2004

Petersen, S.A., R.D. Fetter, J.N. Noordermeer, C.S. Goodman, and A. DiAntonio. 1997. Genetic analysis of glutamate receptors in Drosophila reveals a retrograde signal regulating presynaptic transmitter release. *Neuron*. 19:1237–1248. http://dx.doi.org/10.1016/S0896-6273(00)80415-8

Price, D.A., and M.J. Greenberg. 1977. Structure of a molluscan cardioexcitatory neuropeptide. *Science*. 197:670–671. http://dx.doi.org/10.1126/science.877582

Rathmayer, W., S. Djokaj, A. Gaydukov, and S. Kreissl. 2002. The neuromuscular junctions of the slow and the fast excitatory axon in the closer of the

crab *Eriphia spinifrons* are endowed with different Ca2+ channel types and allow neuron-specific modulation of transmitter release by two neuropeptides. *J. Neurosci.* 22:708–717.

Renden, R.B., and K. Broadie. 2003. Mutation and activation of Galpha s similarly alters pre- and postsynaptic mechanisms modulating neurotransmission. *J. Neurophysiol.* 89:2620–2638. http://dx.doi.org/10.1152/jn.01072.2002

Robb, S., and P. Evans. 1994. The modulatory effect of SchistoFLRFmide on heart and skeletal muscle in the locust *Schistocerca gregaria*. *J. Exp. Biol.* 197:437–442.

Schmidt, H., A. Stonkute, R. Jüttner, D. Koesling, A. Friebe, and F.G. Rathjen. 2009. C-type natriuretic peptide (CNP) is a bifurcation factor for sensory neurons. *Proc. Natl. Acad. Sci. USA*. 106:16847–16852. http://dx.doi.org/10.1073/pnas.0906571106

Schuster, C.M., G.W. Davis, R.D. Fetter, and C.S. Goodman. 1996a. Genetic dissection of structural and functional components of synaptic plasticity. I. Fasciclin II controls synaptic stabilization and growth. *Neuron*. 17:641–654. http://dx.doi.org/10.1016/S0896-6273(00)80197-X

Schuster, C.M., G.W. Davis, R.D. Fetter, and C.S. Goodman. 1996b. Genetic dissection of structural and functional components of synaptic plasticity. II. Fasciclin II controls presynaptic structural plasticity. *Neuron*. 17:655–667. http://dx.doi.org/10.1016/S0896-6273(00)80198-1

Stewart, B.A., H.L. Atwood, J.J. Renger, J. Wang, and C.F. Wu. 1994. Improved stability of *Drosophila* larval neuromuscular preparations in haemolymph-like physiological solutions. *J. Comp. Physiol. A Neuroethol. Sens. Neural Behav. Physiol.* 175:179–191. http://dx.doi.org/10.1007/BF00215114

Tettamanti, M., J.D. Armstrong, K. Endo, M.Y. Yang, K. Furukubo-Tokunaga, K. Kaiser, and H. Reichert. 1997. Early development of the *Drosophila* mushroom bodies, brain centres for associative learning and memory. *Dev. Genes Evol.* 207:242–252. http://dx.doi.org/10.1007/s004270050112

Wan, H.I., A. DiAntonio, R.D. Fetter, K. Bergstrom, R. Strauss, and C.S. Goodman. 2000. Highwire regulates synaptic growth in *Drosophila*. *Neuron*. 26:313–329. http://dx.doi.org/10.1016/S0896-6273(00)81166-6

Wolfgang, W.J., C. Clay, J. Parker, R. Delgado, P. Labarca, Y. Kidokoro, and M. Forte. 2004. Signaling through Gs alpha is required for the growth and function of neuromuscular synapses in *Drosophila*. *Dev. Biol.* 268:295–311. http://dx.doi.org/10.1016/j.ydbio.2004.01.007

Zhong, Y., V. Budnik, and C.F. Wu. 1992. Synaptic plasticity in *Drosophila* memory and hyperexcitable mutants: role of cAMP cascade. *J. Neurosci.* 12:644–651.